

# Mapping trilobite state signatures in atomic hydrogen

Jesús Pérez-Ríos<sup>1</sup>, Matthew T Eiles<sup>1</sup>, Chris H Greene<sup>1,2</sup>

<sup>1</sup>Department of Physics and Astronomy, Purdue University, West Lafayette, Indiana, 47907, USA.

<sup>2</sup> Purdue Quantum Center, Purdue University, West Lafayette, Indiana, 47907, USA.

E-mail: [jperezri@purdue.edu](mailto:jperezri@purdue.edu), [meiles@purdue.edu](mailto:meiles@purdue.edu), [chgreene@purdue.edu](mailto:chgreene@purdue.edu)

March 9, 2021

\*corresponding author

**Abstract.** A few-body approach relying on static line broadening theory is developed to treat the spectroscopy of a single Rydberg excitation to a trilobite-like state immersed in a high density ultracold medium. The present theoretical framework implements the recently developed compact treatment of polyatomic Rydberg molecules, allowing for an accurate treatment of a large number of perturbers within the Rydberg orbit. This system exhibits two unique spectral signatures: its lineshape depends on the Rydberg quantum number  $n$  but, strikingly, is independent of the density of the medium, and it is characterized by sharply peaked features reflecting the oscillatory structure of the potential energy landscape.

*Keywords:* Quantum gases, Ultracold atoms, Rydberg spectroscopy, Quasistatic line broadening theory.

The spectroscopic study of Rydberg atoms in a background gas originated in the outstanding work of Amaldi and Segrè in 1934, who reported a change in the line shape and broadening due to the density and nature of the atomic background gas [1]. Shortly afterwards, Fermi explained these intriguing observations in terms of collisions between the Rydberg electron and neutral atoms (“perturbers”) within its orbit [2]. This theoretical framework predicts the broadening and line shape at a given density to be independent of the Rydberg quantum number  $n$ . Recently, it has become possible to study the spectroscopy of a single Rydberg atom in a high-density environment [3, 4], which has revealed unexpected features of the line shape beyond Fermi’s original framework, such as an  $n$ -dependent shift of the spectroscopic lines [5].

The interaction of the Rydberg electron with a perturber significantly alters the energy landscape of the Rydberg atom. When the electron-perturber interaction is characterized by a negative scattering length this interaction can lead to the formation of long-range molecular states with permanent dipole moments, the so-called trilobite states [6]. These exotic molecules are formed by the mixture of nearly degenerate high angular momentum states, which leads to an oscillating potential energy curve (PEC) extending to thousands of Bohr radii [7]. These molecular states have recently been observed in a thermal gas of Cs [8]. Another exotic state occurs when the electron-perturber interaction possesses a  $p$ -wave scattering resonance, which then produces a different type of molecular state known as a butterfly Rydberg molecule [9]. Very recently this state has been observed in Rb [10].

Two different approaches have been developed to explain the unique features of the Rydberg spectral lines when a single  $nS$  rubidium Rydberg atom is immersed in a dense background gas. One approach describes the line shape in terms of the many-body effects of the background gas [11], whereas the second explains the same physical observables from a few-body perspective by employing the static approximation of line broadening theory [5, 12]. The many-body approach explicitly includes correlation effects within the background gas atoms at finite temperature, leading to a fairly satisfactory explanation of some aspects of the observed line shapes [11]. On the other hand, the quasi-static few-body approach describes other details of the observed line shapes fairly well by sampling the energy shifts in the frozen nuclear Rydberg levels associated with different configurations of the perturbers [5]. This approach readily shows the effect of the Rydberg-neutral PEC in the observed line shapes, and hence it can be a robust technique to probe

and test different Rydberg-neutral PECs within the range of validity of the quasi-static approximation.

The present study explores the spectroscopic line shapes that should be observable for a hydrogen Rydberg atom immersed in a high-density hydrogen background gas. Neglecting corrections due to the spin-orbit interaction, hyperfine splittings, and the Lamb shift, the  $nl$  states of hydrogen are degenerate. The present approach therefore unifies the few-body approach of M. Schlagmüller et al. [5] with the study of polyatomic trilobite states [13]. This requires the inclusion of non-pairwise-additive three, four, etc.  $N$ -body interactions, which were treated only in a pairwise approximation for the  $nS$  states of Rb [4, 5]. Although in hydrogen the triplet and singlet  $e^-$ -H scattering lengths are both positive and therefore no weakly bound Rydberg molecule states form, we nonetheless predict the existence of sharp spectral features at  $n$ -dependent detunings even in the dissociative continuum. Dense hydrogen clouds are attainable in both Bose-Einstein condensate (BEC) [14] and thermal cloud regimes; throughout this paper we present results obtained only for a thermal cloud since these results compare very favorably with identical calculations in the BEC regime.

Fermi’s approach simplifies the interaction between the Rydberg electron and a neutral atom to a contact delta-function potential proportional to the scattering length; this is known as the Fermi pseudopotential [2]. This pseudopotential has been used to study Rydberg-neutral interactions with considerable success [15, 16]. Extending this model to a Rydberg hydrogen atom in the presence of  $N$  neutral hydrogen atoms placed at positions  $\vec{R}_i$  within the Rydberg blockade radius gives a potential energy (in atomic units) [17]:

$$V = 2\pi \sum_{i=1}^N A_{S,T}(R_i) \delta^3(\vec{r} - \vec{R}_i), \quad (1)$$

where  $A_{S,T}(R_i)$  denotes the energy-dependent singlet ( $S$ ) and triplet ( $T$ ) scattering lengths [18]:

$$A_{S,T}(R) = A_{S,T}^0 \left[ 1 - \frac{\pi\alpha_d k}{3A_{S,T}^0} - \frac{4\alpha_d}{3} k^2 \ln \left( \frac{\sqrt{\alpha_d k}}{4} \right) \right]^{-1}.$$

The semiclassical momentum is  $[k(R)]^2 = 2/R - 1/n^2$  and the static polarizability of hydrogen is  $\alpha_d = 9/2$ . The scattering lengths at zero energy are  $A_S^0 = 5.965 a_0$  and  $A_T^0 = 1.7686 a_0$  [19]. The present study concentrates on triplet spin states because they can be readily explored in a spin-polarized BEC. Previous work has shown that this pseudopotential agrees qualitatively with more sophisticated potentials

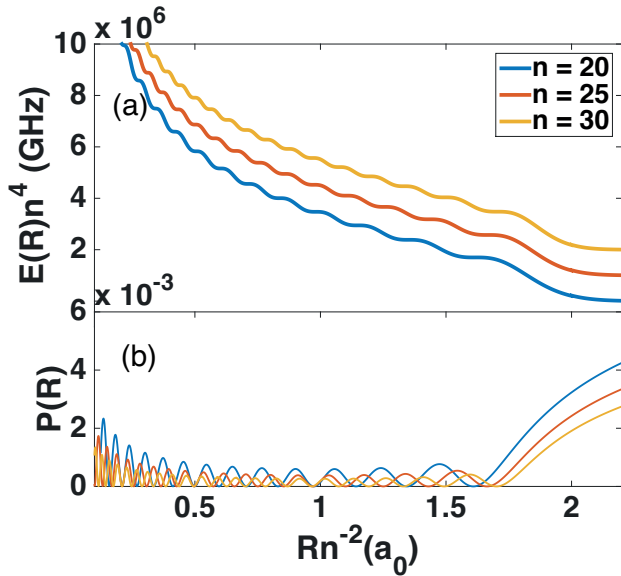


**Figure 1.** Panel (a): diatomic potential energy curves  $E(R)$  in GHz for different triplet Rydberg states of hydrogen,  $H(n)+H(1s)$ , plotted in scaled coordinates and spaced vertically by  $10^6$  in these scaled units for clarity. The step-like structure of these potentials similarly arises in calculations of singlet  $H(n)+H(1s)$  potential energy curves [18]. Panel (b): probability of two-photon excitation  $\mathcal{P}(R) = |\langle nD|\Psi_T\rangle P_D^n + \langle nS|\Psi_T\rangle P_S^n|^2$ , integrated over angular degrees of freedom as a function of the distance (see text for details) for the same Rydberg states of panel (a).

at low  $n$ , and its accuracy increases to a quantitative level for higher Rydberg levels [15, 16, 18, 20].

Treating the interaction potential as a perturbation of the degenerate hydrogenic states  $\psi_{nlm}(\vec{r}) = \frac{u_{nl}(r)}{r} Y_{lm}(\hat{r})$  with principal Rydberg quantum number  $n$  and orbital angular momentum  $l$  with projection  $m_l$ , the energy shift can be obtained in standard degenerate perturbation theory. This becomes computationally cumbersome since the number of states scales as  $n^2$ . However, the first order normalized perturbed eigenstates - the trilobite states - of a delta function potential are analytically known:

$$\Psi(\vec{R}_i, \vec{r}) = \frac{1}{\mathcal{N}} \sum_l \frac{u_{nl}(R_i)}{R_i} \frac{u_{nl}(r)}{r} \frac{2l+1}{4\pi} P_l(\hat{R}_i \cdot \hat{r}); \quad (2)$$

$$\mathcal{N}^2 = \Psi(\vec{R}_i, \vec{R}_i),$$

and have been employed in a recent approach as a reduced basis to diagonalize Eq. (1) [13]. This reduces the dimensionality of the problem to at most  $N$ , the number of perturbers, and is exact for hydrogen within the approximation of degenerate perturbation theory. This leads to a generalized eigenvalue problem

$$\mathbf{A}\vec{a} = E\mathbf{B}\vec{a};$$

$$\mathbf{A}_{\alpha\beta} = 2\pi \sum_i A_T(R_i) \Psi^*(\vec{R}_\alpha, \vec{R}_i) \Psi(\vec{R}_i, \vec{R}_\beta), \quad (3)$$

where  $\mathbf{B}_{\alpha\beta} = \Psi(\vec{R}_\alpha, \vec{R}_\beta)$  and  $\mathbf{A}$  is the coupling matrix of trilobite states centered at different perturbers [13]. The off-diagonal elements are proportional to the overlap between trilobite wavefunctions localized on different perturbers and account for the non-additive pair-wise nature of the Rydberg-neutral interaction when multiple perturbers lie within the Rydberg orbit. Each of the  $N$  nonzero eigenvalues of this expression defines an  $3N$ -dimensional potential energy surface; the  $k$ th- eigenenergy corresponds to the eigenstate

$$\Psi_k(\{\vec{R}_i\}, \vec{r}) = \frac{1}{\mathcal{N}} \sum_i a_{ik} \Psi(\vec{R}_i, \vec{r}); \quad (4)$$

$$\mathcal{N}^2 = \sum_{i,j} a_{ik} a_{jk} \Psi(\vec{R}_i, \vec{R}_j).$$

For the single-perturber case the sole non-zero eigenenergy is given in closed form: [21]

$$E(R) = 2\pi A_T(R) \Psi(R, R) \quad (5)$$

$$= 2\pi A_T(R) [u_{n0}(R) Y_{00}(\hat{R})]^2 ([k(R)]^2 + [Q(R)]^2);$$

where  $Q(R) = u'_{n0}(R)/u_{n0}(R)$ . The potential energy curves for a single perturber within the Rydberg orbit are shown in Fig. 1a, which shows the oscillatory structure of the potentials. Some of the oscillations exhibit local minima in  $E(R)$  due to the energy dependent nature of the phase-shift.

We propose a two-photon excitation scheme from the spin-polarized  $1S$  ground state to either of the  $nS$  or  $nD$  Rydberg states, both of which are allowed by selection rules, using two counter-propagating, linearly-polarized beams with  $\lambda \approx 181$  nm. With this excitation scheme the momentum kick of the photons to the atom will be negligible. The transition amplitudes for these two different routes, denoted as  $P_S^n$  and  $P_D^n$ , respectively, have been calculated using a Sturmian basis set leading to accurate results (within  $\sim 10\%$ ) in comparison with other approaches [26, 27]. We have calculated  $P_S^{20} = -0.11$ ,  $P_D^{20} = 0.48$ ; the ratio of these values changes by less than 10% for  $n = \infty$ . We have therefore assumed these values for all  $n$  [28]. The trilobite state can be excited via its  $nS$  or  $nD$  character, depending on the nature of the Rydberg state. When a single perturber is present the probability of excitation, allowing for both pathways and averaged over the relative angle between the internuclear axis and the quantization axis, is:

$$\mathcal{P}(R) = (4\pi)^{-1} \int d\Omega |\langle nD|\Psi_T\rangle P_D^n + \langle nS|\Psi_T\rangle P_S^n|^2$$

$$= \frac{(P_S^n)^2 + \left(\frac{u_{n2}(R)}{u_{n0}(R)} P_D^n\right)^2}{R^2([k(R)]^2 + [Q(R)]^2)}. \quad (6)$$

The probability of excitation as a function of the distance for different Rydberg states are shown in

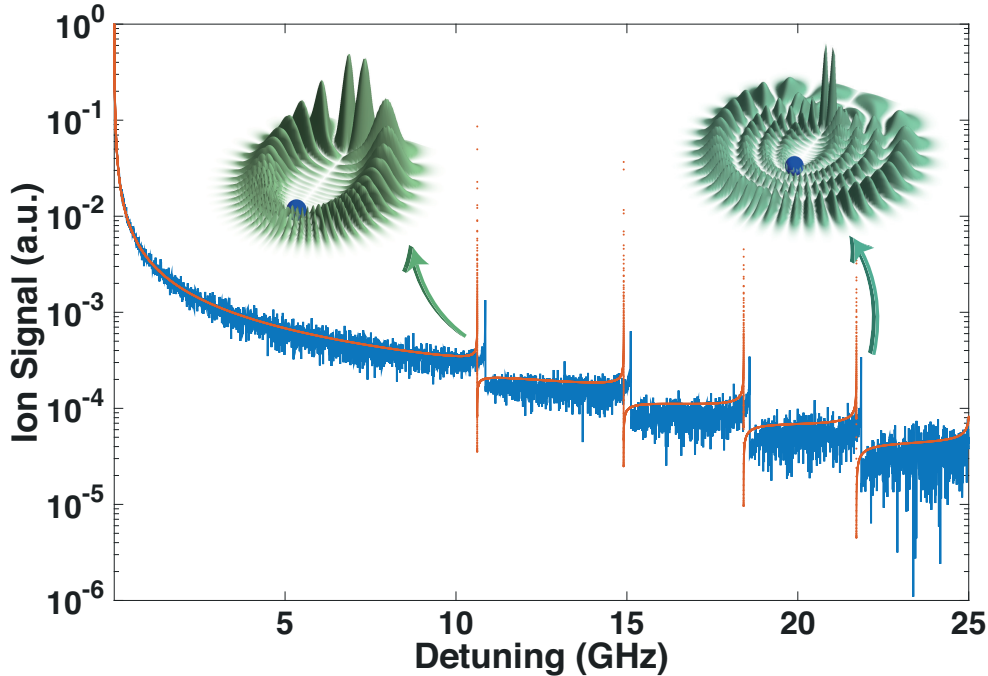


**Figure 2.** Normalized spectra of a single hydrogen Rydberg atom with  $n = 20$  in a high density background gas of hydrogen at  $\rho = 10^{15} \text{ cm}^{-3}$ . Only detunings higher than 25 MHz, where the quasistatic approximation is accurate, are shown. The quasistatic results for the line shape is depicted by the solid blue line, whereas the red line represents the line shape assuming a two-body quasistatic approach (see Eq. 10 in the text for details). Each of the peaks of the spectra correlates with the existence of local extrema in the Rydberg-perturber interaction potential.  $5 \times 10^6$  Monte Carlo events have been employed in this simulation.

Fig. 1b. These show an oscillatory behavior related to the  $nD$  and  $nS$  hydrogenic wave functions, but tend towards a constant for large perturber-Rydberg distance. For multiple perturbers, the probability to excite the  $k$ th eigenstate is given by

$$\begin{aligned} \mathcal{P}^k(\{\vec{R}_i\}) &= \\ & \sum_i a_{ik} \left| P_S^n \langle nS | \Psi(\vec{R}_i, \vec{r}) \rangle + P_D^n \langle nD | \Psi(\vec{R}_i, \vec{r}) \rangle \right|^2 \\ &= \frac{\left[ \sum_i a_{ik} \left( P_D^n \psi_{n20}(\vec{R}_i) + P_S^n \psi_{n00}(\vec{r}_i) \right) \right]^2}{\sum_{i,j} a_{ik} a_{jk} \Psi(\vec{R}_i, \vec{R}_j)}. \end{aligned} \quad (7)$$

The spectroscopy of a single Rydberg hydrogen atom in an ultracold background gas of hydrogen is modeled assuming the quasistatic theory of line broadening [12, 22, 23, 24]. In this theory, the absorber (the Rydberg atom) is assumed to be at rest and absorbs photons at  $\omega_0 + \Delta\omega$ , where  $\omega_0$  is the frequency between the two states of the Rydberg atom and  $\Delta\omega$  accounts for the shift of the involved levels by the perturbing potential of the neighboring atoms. An additional assumption is that only the perturbers located in a given interacting region, which in the present case is the volume of the Rydberg atom,  $V_{Ryd}$ , will contribute to the line broadening.

The quasistatic picture for the line broadening breaks down when the collision time is close to or less than the inverse detuning,  $\tau_c \sim 1/\Delta\omega$  [24, 25]. In this regime the Rydberg-perturber collisions give the major contribution to the line broadening. The collision time can be estimated as  $\tau_c = b/\langle v \rangle$ , where the impact parameter  $b$  is assumed to be of the same order of magnitude as the Rydberg orbit size, *i.e.*,  $b \sim 2n^2$ . Considering a thermal cloud of hydrogen at  $T \sim 50 \text{ } \mu\text{K}$ ,  $\tau_c \sim 20 - 200 \text{ ns}$ . Thus, for a thermal cloud of hydrogen the line shapes in the range  $\Delta\omega \gtrsim 25 \text{ MHz}$  can be approximated by the quasistatic approach.

The simulations of the line profile are performed following the method of Schlagmüller et al. [5]. In a homogeneous gas of density  $\rho$ , the probability of finding a certain number of atoms in the volume of the Rydberg atom defines a Poisson distribution with a mean number  $\langle N \rangle = \rho V_{Ryd}$ , where  $\langle N \rangle$  denotes the average number of perturbers in the Rydberg volume. This Poissonian distribution is employed to sample uniformly the  $N$  atoms within the Rydberg volume. For the  $i$ -th sample of the number of perturbers in the Rydberg orbit, the target Rydberg state experiences an energy shift  $E_j$ ; each of these energies are then weighted by the probability of the excitation of the given configuration. Finally the line shape is given

by the  $\mathcal{P}$ -weighted distribution of calculated energies in each of the samples,  $S(E)$ . In the present work the reported spectra are presented in terms of the ion signal since an ionization detection technique is assumed, as is commonly utilized in the field. The spectra are normalized to unity with respect to the highest signal at small detunings.

The spectrum of a single hydrogen Rydberg atom with  $n = 20$  in a dense and ultracold gas is shown in Fig.2, which prominently displays the existence of certain sharp spectral features following a quasi-periodic pattern in terms of the detuning of the excitation field. This pattern is intimately related with the underlying PEC; in particular, each of the peaks reflects the existence of a plateau in the potential energy landscape (see Fig.1). In each of these plateaus the Rydberg electron is repeatedly elastically scattered by, primarily, just one of the perturbing atoms, leading to a trilobite-like wave function for the Rydberg-perturber system [6]. At each plateau, as the detuning increases, an angular node is exchanged for an additional radial node such that the total number of nodes remains a constant integer value at each plateau. This reflects the fact that, at each plateau, the electronic wave function is predominantly characterized by a single elliptical eigenstate [7]. These wave functions are displayed in Fig. 2, where the Rydberg core is depicted by the blue ball whereas the perturber is placed underneath the electron density maximum. Therefore, the line shape of the Rydberg spectrum directly maps the Rydberg-perturber PEC, leading to a very robust spectroscopic method for observation of this system.

A simple model for the lineshape, assuming that only a single perturber lies in the Rydberg orbit, conveys significant physical intuition about the system's lineshapes and spectral features. This has been shown in the case of long-range forces by Kuhn [22, 23]. This assumption is clearly more accurate for dilute gases or low Rydberg excitations, but is also a valuable limiting case for the many-perturber scenario and qualitatively displays some of the same features. For a given density  $\rho$  the probability to find a single perturber between distances  $R$ ,  $R + dR$  from the ion is given by the nearest neighbour distribution,

$$P(R) = \frac{3}{\Delta} \left(\frac{R}{\Delta}\right)^2 e^{-(R/\Delta)^3}, \quad \Delta = (4\pi\rho/3)^{-1/3}. \quad (8)$$

This distribution must be additionally modified to include the radial dependence of the radial probability of exciting the trilobite state, i.e. the probability distribution is that of Eq. 8 multiplied by Eq. 6:

$$P(R) = \frac{3e^{-(R/\Delta)^3} \left[ (P_S^n)^2 + \left( P_D^n \frac{u_{n2}(R)}{u_{n0}(R)} \right)^2 \right]}{\Delta^3 ([k(R)]^2 + [Q(R)]^2)}.$$

The line shape is then given by converting this into a probability distribution with respect to the energy via the relationship  $|P[R(E)]dR| = |P(E)dE|$ . This introduces the derivative of the potential energy, which can be calculated analytically:

$$\frac{dE}{dR} = \frac{dV(R)}{dR} = -A_T(R) \left( \frac{u_{n0}(R)}{R} \right)^2 + \frac{A'_T(R)[u_{n0}(R)]^2}{2} ([k(R)]^2 + [Q(R)]^2) + \frac{2\alpha_d}{R^5}.$$

Upon inverting the PEC to obtain  $R$  as a function of the detuning, denoted  $R_E = R(E)$ , the line shape for the situation of a single perturbing atom within the Rydberg orbit is given by

$$P(E) = \frac{3e^{-(R_E/\Delta)^3} \left[ (P_S^n)^2 + \left( P_D^n \frac{u_{n2}(R_E)}{u_{n0}(R_E)} \right)^2 \right]}{\Delta^3 ([k(R_E)]^2 + [Q(R_E)]^2)} \left| \frac{dE}{dR_E} \right|^{-1}. \quad (9)$$

This expression compactly separates into two factors. The first, a broad background, is given by the first factor of Eq. 10. The second contains the peak structure and is unity for nearly all detunings except at the detunings of the series of sharp doublet peaks, and is given by the second factor of Eq. (10):

$$P(E) = \left( \frac{3 R_E^2 e^{-(R_E/\Delta)^3}}{2 \Delta^3 E} \right) \cdot \left( \frac{\left[ (P_S^n)^2 + \left( P_D^n \frac{u_{n2}(R_E)}{u_{n0}(R_E)} \right)^2 \right]}{1 - \frac{1}{A_T(R_E)[u_{n0}(R_E)]^2} \left( \frac{A'_T(R_E)}{A_T(R_E)} R_E^2 E + \frac{2\alpha_d}{R_E^3} \right)} \right). \quad (10)$$

The smooth background given by the first factor can also be obtained by considering the approximate PEC derived by Borodin and Kazansky [29]. The asymptotic limits for small and large detunings of the functional form in Eq. (10) establishes the power-law scaling of the lineshapes, previously introduced by Kuhn for the case of van der Waals forces [22, 23]. For small detunings, corresponding to large  $R$ , the potential is very insensitive to  $R$  and so the inverse function  $R_E$  is nearly constant. The first factor in Eq. 10 is therefore proportional to  $E^{-1}$ , and the second is unity in this limit. A power law fit to the simulated lineshapes over an energy range from zero to the location of the first peaks gives  $E^{-0.86 \pm 0.01}$ , quite independently of density and the Rydberg state. This change in the power law, along with the small constant shift in the location of the doublet peak structure in Fig. 2, indicate the expected deviation beyond the single-perturber model.

At large  $E$ , corresponding to fairly low  $R$ , the radial wavefunction  $[u_{n0}(R)]^2$  increases roughly

proportional to  $R^{1/2}$ ; the modulating factor  $k^2 + Q^2$  introduces a factor  $R^{-1}$  making the leading order dependence of the potential curve for small  $R$  (but not so small as for the polarization potential to dominate yet)  $E \sim R^{-1/2}$ . Inverting then gives  $R \sim E^{-2}$ , so that  $P(E) \sim E^{-5}$ . This is a good estimate for the power law behavior in this regime, which numerical fits typically match well with  $P(E) \sim E^{-4} - E^{-5}$ , for detunings greater than  $\sim 10$  GHz for  $n = 30$ . This power law behavior is of course only satisfied when the second factor is unity; near the peak regions this term dominates.

An analysis of the components of equation (9) explains the locations and shape of these sharp peaks in the spectra. For clarity throughout this discussion, we ignore the energy dependence of the scattering length and the polarization potential, so that  $|dE/dR_E|^{-1} = |A_T(R)(u_{n0}(R)/R)^2|^{-1}$ . This clearly demonstrates that the peaks in the spectrum stem from the plateaus of the potential energy curve. These are located at the nodes of the  $s$ -wave radial wave function. The first factor of eqn. (9) also depends on  $R_E$  in a complicated fashion, but near the nodes of  $u_{n0}(R_E)$  it behaves as  $[P_S^n u_{n0}(R_E)]^2 + [P_D^n u_{n2}(R_E)]^2$ . If only the  $S$  component was excited, the  $u_{n0}(R_E)$  factors would cancel and the spectrum would no longer exhibit peaks. However, the  $nD$  component is proportional to the ratio  $u_{n2}(R_E)/u_{n0}(R_E)$  and thus vanishes at the node of the  $d$ -wave radial wave function very near the peak due to the node of the  $s$ -wave radial wave function, leading to the asymmetric profile seen in Figs. (2) and (3) where a sharp peak is immediately followed by a step-like drop in the line shape. Inclusion of the energy dependence of the scattering length in fact allows the  $nS$  character to exhibit peaks since it slightly offsets the location of the inflection points of the potential curve from the location of the  $s$ -wave radial nodes, but this effect is mostly overwhelmed by the dominant  $nD$  character.

The dependence of the lineshape on density is another fascinating feature of this system. The spectrum of a single Rydberg hydrogen atom with  $n = 30$  immersed in a perturbing gas as a function of its density is displayed in Fig.3a. The line shape is found to be independent of the density of the perturbing gas. These results seem to contradict the established line broadening theory which predicts a linear dependence of the line broadening with respect to the density of the perturbing gas [24], since higher numbers of perturbers lead to larger shifts of the excited levels involved in the absorption process. However, the special nature of this system shows that the effect of different perturbers is clearly non-additive [13]. In particular, for  $N$  perturbers,  $N$  eigenenergies of Eq. 1 split about the single-perturber eigenenergy,

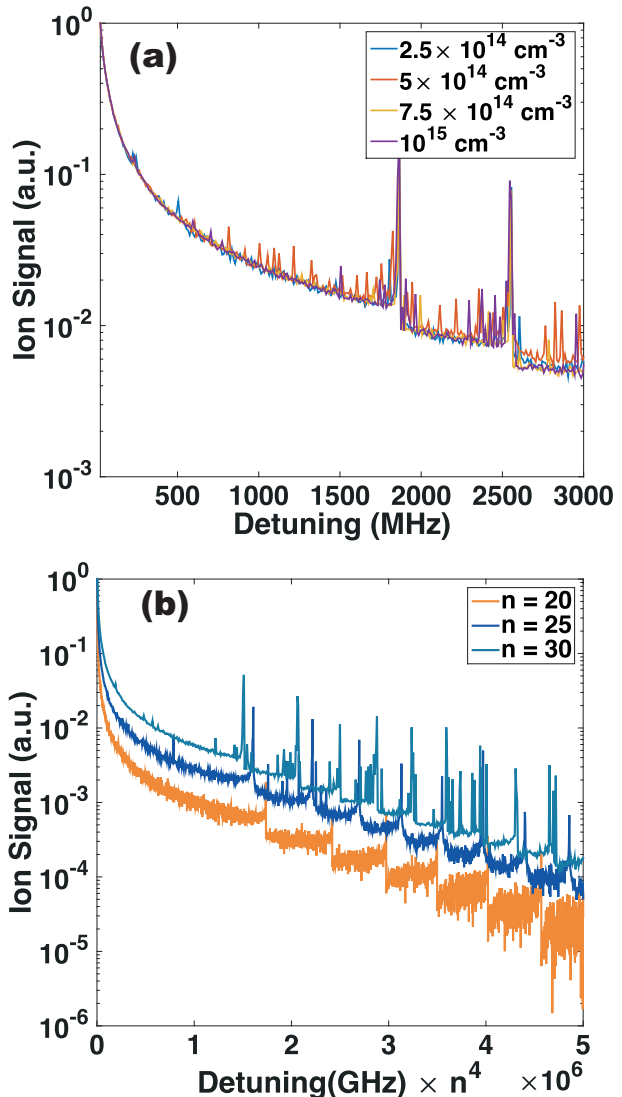


**Figure 3.** Normalized spectra of a single hydrogen Rydberg atom in a thermal gas at ultracold temperatures. The Rydberg spectra for  $n = 30$  and different densities is shown in panel (a).  $10^6 - 5 \times 10^5$  Monte Carlo events were simulated, with the number of events decreasing as the density increases. The spectrum for  $\rho = 10^{15} \text{ cm}^{-3}$  for different Rydberg states is shown in panel (b). The horizontal axis has been scaled by  $n^4$  as in Fig. 1 to emphasize the regular spacing of the peaks and the increased number of peaks per unit detuning as  $n$  increases.  $5 \times 10^6$  events were simulated for  $n = 20$  and  $8 \times 10^5$  for  $n = 25, 30$

and so on average the contributions from higher-energy potential energy curves will be counteracted by contributions from lower-lying curves; as a result the line shape should be independent of the number of perturbing atoms and only depend on the Rydberg state. Indeed, this is numerically corroborated in Fig.3b, where the spectrum for a given density and different Rydberg states is shown. These results will no longer apply when the probability of finding at least

one perturber within the Rydberg orbit is substantially smaller than one, or else so high that the number of perturbing atoms exceeds the number of states available to construct the trilobite state,  $n^2$ . These two limits set the range of applicable densities at  $\langle N \rangle \sim 0.1 \leq \frac{32\pi n^6}{3} \rho \leq n^2$ . Within these limits, this system would be the first, to our knowledge, to exhibit a lineshape independent of the density.

The dependence on  $n$  has also been explored: the Rydberg spectrum of a single Rydberg excitation in a dense background gas as a function of the Rydberg state has been calculated within the quasistatic approach of the line broadening and the results are shown in Fig.3b. for three Rydberg states at the same density. These lineshapes possess the expected regular series of peaks, which can be correlated with those in Fig. 1. They show the same overall behavior as expected based on the potential energy curves, especially in that they exhibit the same regular scaling,  $n^4$ , as the potential energy curves.

In this work a generalization of the quasistatic line broadening theory has been applied for the Rydberg excitation spectra of a single Rydberg hydrogen atom immersed in a high-density background hydrogen gas. The simulations not only account for the position and energy shift due to the perturbers, but also the probability of excitation of different atomic configurations by means of the  $S$  and  $D$  character of the target state. As a result, Rydberg hydrogen atoms immersed in a dense background gas of hydrogen will show a quasi-periodic series of peaks in the line shape correlating with the fundamental nature of the underlying Rydberg-neutral interaction. In particular, the positions of these peaks relate closely to the locations of the plateaus in the potential curves, which depend sensitively on the calculated energy dependent electron-hydrogen scattering lengths. Thus, our findings clearly indicate the possibility to use direct line shape data to explore the Rydberg-perturber energy landscape.

The calculated spectra clearly show a positive detuning in relation with the repulsive nature of the Rydberg-perturber interaction, as well as a density independent line shape, in stark contrast with the conventional line broadening theory, which predicts a linear density dependence of the line shift and line broadening. These findings have been explained by appealing to the unusual and intriguing properties of the polyatomic trilobite-like states, suggesting a consistent and convincing explanation of the spectra.

Rydberg states are also present in astrophysical spectra, where even  $n = 1000$  and higher have been observed [30, 31]. Although these Rydberg states form in very dilute interstellar clouds where the interatomic spacings are very large, trilobite states could form for

very high  $n$ . The theory developed here could be applied to explain some aspects of the recombination lineshape due to the effect of a nearby neutral atom.

## Acknowledgments

This work is supported in part by the National Science Foundation under Grant No. PHY-1306905. We appreciate the assistance and help of M. Schlagmüller in the many-body simulations for the line broadening, as well as fruitful discussions with F Robicheaux.

## References

- [1] Amaldi E and Segrè E (1934) *Nature* (London) **133**, 141
- [2] Fermi E 1934 *Nuovo Cimento* **11**, 157
- [3] Balewski J B, Krupp A T, Gaj A, Peter D, Büchler H P, Löw R, Hofferberth S and Pfau T (2013) *Nature* (London) **502**, 664
- [4] Gaj A, Krupp A T, Balewski J B, Löw R, Hofferberth S and Pfau T 2014 *Nat. Commun.* **5**, 4546
- [5] Schlagmüller M, Liebisch T C, Nguyen H, Lohead G, Engel F, Böttcher F, Westphal K M, Kleinbach K S, Löw R, Hofferberth S, Pfau T, Pérez-Ríos J, Greene C H 2016 *Phys. Rev. Lett.* **116** 053001.
- [6] Greene C H, Dickinson A S and Sadeghpour H R 2000 *Phys. Rev. Lett.* **85**, 2458
- [7] Granger B, Hamilton E L and Greene C H 2001, *Phys. Rev. A* **64** 042508.
- [8] Booth D, Rittenhouse S T, Yang J, Sadeghpour H R, & Shaffer J P 2015 *Science*, **348**, 99.
- [9] Hamilton E L, Greene C H and Sadeghpour H R 2002 *J. Phys. B* **35**, L199
- [10] Niederprüm T, Thomas O, Eichert Lippe C, Pérez-Ríos J, Greene C H 2016 arXiv:1602.08400v1
- [11] Schmidt R, Sadeghpour H R and Demler E 2015 *Phys. Rev. Lett.* **116**, 105302.
- [12] Collins II W G, *The Fundamentals of Stellar Astrophysics*, 2003
- [13] Eiles M T, Pérez-Ríos J, Robicheaux F and Greene C H 2016 *J. Phys. B* **49**, 114005.
- [14] Fried D G *et al* 1998 *Phys. Rev. Lett* **81** 3811; see also Killian T C *et al* 1998 *Phys. Rev. Lett.* **81** 3807.
- [15] Du N Y and Greene C H 1987 *Phys. Rev. A* **36** 971(R); (erratum: **36** 5467).
- [16] de Prunelé, E 1987 *Phys. Rev. A* **35** 496; (erratum: **35** 4864.)
- [17] Liu I C H and Rost J M 2006 *Eur. Phys. J. D* **40**, 65
- [18] Tarana M and Curik R 2016 *Phys. Rev. A* **93** 012515
- [19] Schwartz C 1961 *Phys. Rev.* **24** 1468.
- [20] Dickinson A S and Gadea F X 2002 *Phys. Rev. A* **65**, 052506
- [21] Chibisov M, Ermolaev A M, Brouillard F, and Cherkani M H 2000 *Phys. Rev. Lett.* **84**, 451; see also Cherkani M H, Brouillard F, and Chibisov M 2001 *J. Phys. B.* **34** 49.
- [22] Kuhn H 1934 *Phil. Mag.* **18**, 987
- [23] Kuhn H 1937 *Proc. Roy. Soc. A* **158**, 212; see also Kuhn H 1937 *Proc. Roy. Soc. A* **158**, 230
- [24] Allard N and Kielkopf J 1982 *Rev. Mod. Phys.* **54**, 1103
- [25] Holstein T 1950 *Phys. Rev.* **79**, 744
- [26] Quattropani A, Bassani F and Carillo S 1980 *Phys. Rev. A* **25**, 3079
- [27] Joshi, R 2006 *Phys. Lett. A* **361**, 352
- [28] Florescu V, Patrăscu, and Stoican O 1987 *Phys. Rev. A* **36**, 2155.
- [29] Borodin V M and Kazansky A K 1992 *J. Phys. B.* **25** 971.

- [30] Dalgarno A 1983 *Rydberg States of Atoms and Molecules* ed Stebbings R F and Dunning F B (Cambridge: Cambridge University Press)
- [31] Stepkin S V, Konovalenko A A, Kantharia N G, and Udaya Shankar N 2007 *Mon. Not. R. Astron. Soc.*, 374:852.